Journal of Alloys and Compounds 488 (2009) 425–429

Contents lists available at ScienceDirect

Journal of Alloys and Compounds

journal homepage: www.elsevier.com/locate/jallcom

Comparison of levitation force relative to thickness of disk shaped $YBa_2Cu_3O_{7-x}$ prepared by MPMG and FQMG processes

S. Kütük, S. Bolat*, M. Başoğlu, K. Öztürk

Department of Physics, Faculty of Arts and Science, Karadeniz Technical University, 61080 Trabzon, Turkey

ARTICLE INFO

Article history:
Received 10 July 2009
Received in revised form 21 August 2009
Accepted 24 August 2009
Available online 8 September 2009

Keywords:
Y123
Melt process
Levitation force
Volume fraction

ABSTRACT

The precursor YBCO in the stoichiometric ratio of 1:2:3 were fabricated using the melt-powder-melt-growth (MPMG) technique, and flame-quench-melt-growth (FQMG) technique. The superconducting regions were determined by calculating the levitation force per unit volume as a function of samples' thickness. Our findings indicate that superconductivity forming ratio is sensitive to the preparation techniques and it grows on the surfaces of the samples prepared by FQMG process while it grows in the middle of the samples fabricated by MPMG technique. It was determined that the MPMG process produces more the superconductivity forming ratio than the FQMG method, which is due to platinum impurities. Our results were also checked by polarized optical microscope and XRD pattern.

1. Introduction

Magnetic levitation force due to the interaction between a permanent magnet and T_c superconductors (HTS) is an important measurement to determine superconductivity forming ratio and is very sensitive several factors in experiments. Perhaps, the most important factor is the sample preparation technique such as solid state reaction (SSR) technique, ammonium nitrate (AN) technique, and melt-growth (MG) techniques. Among these techniques, melting techniques appear to produce higher critical current density (J_c) and irreversibility magnetic field (H_{irr}). Jin et al. [1] proposed the melt-textured-growth (MTG) process for $YBa_2Cu_3O_{7-x}$ (Y123). Murakami et al. [2] developed the quench-melt-growth (QMG) technique in which Y_2BaCuO_5 (Y211) particles and their dispersion can be controlled. Later, Murakami et al. [3] improved this technique so called melt-powder-melt-growth (MPMG) process. In order to fabricate HTS, various methods such as powder-melt-process (PMP) [4], top-seeded-melt-growth (TSMG) [5], the solid–liquid-melt-growth (SLMG) [6], and the flame-quench-melt-growth (FQMG) [7] have been developed.

Another parameter affecting the levitation force is the size of samples. The studies revealed [8,9] that the levitation force increases linearly with increasing the thickness of the samples but it reaches a constant value after a certain thickness. Alqadi et al. [10] suggested that the levitation force per unit volume increases exponentially with decreasing the thickness of samples. However, because of limited theoretical and experimental studies, the influence of the size of the sample on the levitation force is not clear yet.

In this study, we prepared YBCO in the stoichiometric ratio of 1:2:3 using the MPMG and FQMG processes and measured them magnetic levitation force as a function of the samples' thickness. We determined that superconductivity forming ratio is sensitive to the preparation techniques and it grows (it dominates) on the surfaces of the samples prepared by FQMG while it grows (it dominates) in the middle of the samples fabricated by MPMG. The MPMG process produces more the superconductivity forming ratio than the FQMG method, which due to platinum impurities. Our findings will be helpful in designing and manufacturing the practical application YBCO in the stoichiometric ratio of 1:2:3 systems based on the magnetic levitation force.

2. Experimental procedure

In order to fabricate precursor YBCO bulk materials, we used Y_2O_3 (99.99% purity), $BaCuO_3$ (99.98% purity) and CuO (99.99% purity) powders. These powders were first mixed in the stoichiometric ratios of 1:2:3 compositions. Mixed powders were well reground using a planar ball milled machine model of Retsch PM100. Then, these powders were put into alumina crucible and then they were calcined at 915 °C for 24 h in air in an 818 Euroterm Controller/Programmer Muffle furnace. After that, our samples were prepared by using two different melting methods. First method was MPMG process and details about its preparation have been described in Ref. [3]. In this technique, we made some changes in the quench procedure. As shown in Fig. 1a, the material in platinum crucible was dwelled at 1460 °C for 5 min, and then it was suddenly placed to liquid nitrogen dewar. The molten material was reground well and then it was compressed into pellet form using a pressure of 300 MPa on a 13 mm diameter. This material was sintered a tube furnace in air at reached maximum temperature 1125 °C (sample A) as seen Fig. 1b.

* Corresponding author. Tel.: +90 462 3772537; fax: +90 462 3253195.
E-mail address: sbolat@ktu.edu.tr (S. Bolat).

0925-8388/$ – see front matter
doi:10.1016/j.jallcom.2009.08.149

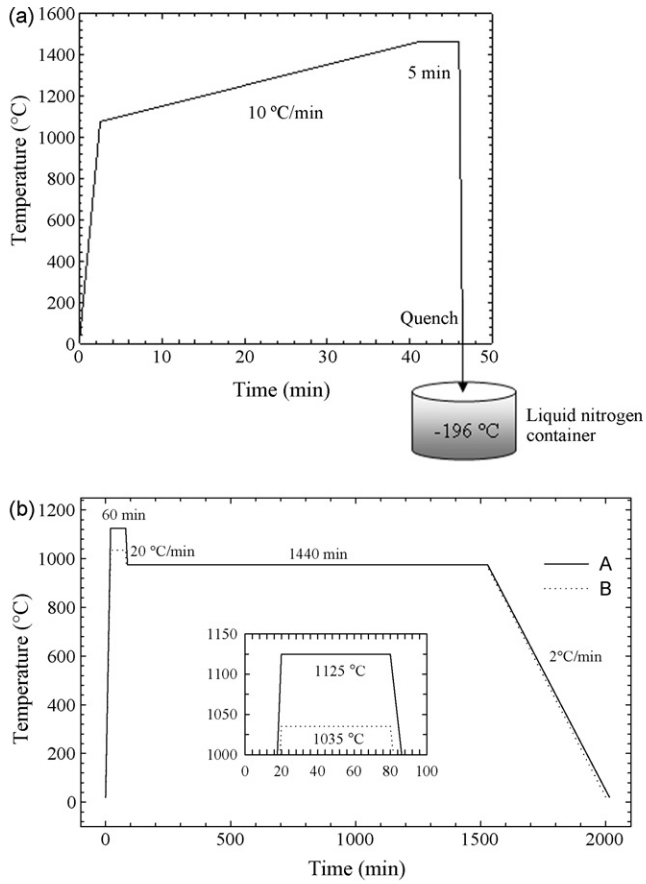

Fig. 1. Diagram of (a) quench process for MPMG and (b) sintering for MPMG and FQMG.

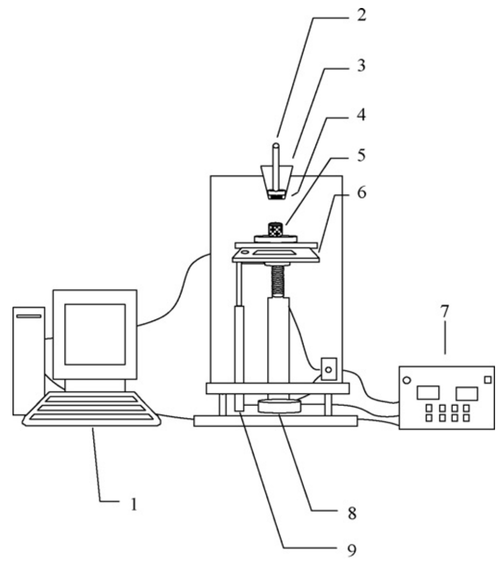

Fig. 2. Scheme of the measurement system of high-temperature superconducting magnetic force: (1) computer, (2) sample holder, (3) liquid nitrogen vessel, (4) superconducting sample, (5) Nd–Fe–B magnet, (6) electronic balance, (7) control device, (8) servomotor, and (9) displacement sensor.

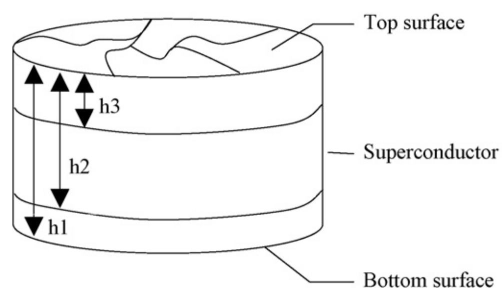

Fig. 3. Scheme for thickness of superconductor.

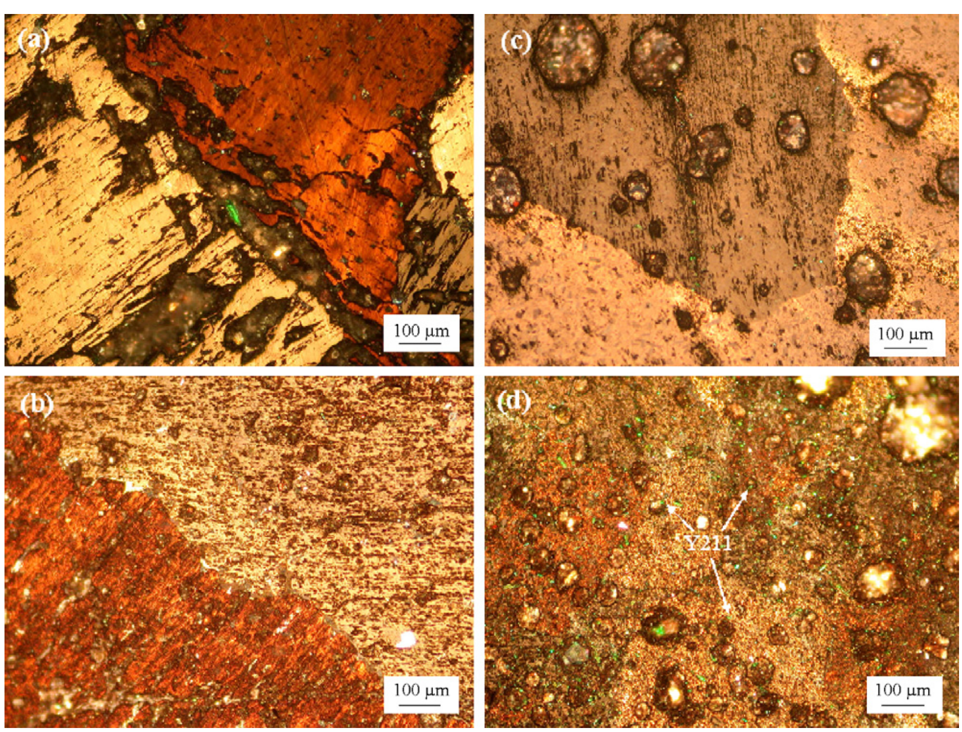

Fig. 4. Polarization optical micrographs of both melting process and thickness of superconductor for (a) A-h1, (b) A-h2, (c) B-h1, and (d) B-h2.

In the second approach, we used the standard FQMG technique [7]. We first quenched the sample and then followed exactly the same procedures as in MPMG method; the maximum temperature reached was 1035 °C for the sample B as shown in Fig. 1b. Then, both of them were annealed in flowing oxygen at 450 °C for 2 h.

The surface morphology of the samples was examined by using Nikon ECLIPSE ME 6000 polarized optical microscope with 300× magnitude. The X-ray diffraction (XRD) data were obtained using a Rigaku D/Max-IIIC diffractometer with Cu Kα radiation over the range of 20–60° with a scan speed of 0.2° min^{-1} at room temperature.

The energy dispersive X-ray fluorescence technique (EDXRF) was used to determine the amount of platinum (Pt) contaminated in the sample A during quench process for MPMG. YBCO compounds were excited with an annular Co-57 radioactive source whose radioactivity is 925 MBq emitting 123.6 keV photons. The characteristic emitted X-ray with 5.96 keV energy resolutions was counted by an Ultra-LeGe detector.

The magnetic levitation force was determined by a computer controlled experimental set up as shown in Fig. 2. The levitation force under zero-field-cooled (ZFC) regime and at the liquid temperature (77 K) was measured as a function distance between a superconductor and a cylindrical Nd–Fe–B magnet having a 30 mm diameter and a 30 mm height. While magnetic field intensity at the center of the top surface of PM with axial magnetic field intensity is 550 mT, the intensity of magnetic field was found to be 440 mT at the closest distances of 3 mm.

In order to understand the influences of precipitate phases formed in the samples on the levitation force, the disk shaped sample surfaces were sandpapered to change the thickness of the samples. These thicknesses shown in Fig. 3 were named as h1, h2 and h3 (the values of h1, h2, and h3 are 6.2, 5.5, and 2.5 for MPMG and 4.1, 3.8, and 2.3 mm for FQMG samples).

3. Results and discussion

Fig. 4 shows optical micrographs as a function of the thickness of $YBa_2Cu_3O_{7-x}$ samples fabricated by both MPMG and FQMG. This figure clearly indicates that the surface morphology of the samples depends on the samples' thickness as well as melting processes. As can be clearly seen from Fig. 4a, the top surface of the sample A with an h1 thickness has large grains with textured Y123 crystals. The boundaries between the large Y123 grains were not clean and the weak-link between grains can be obviously seen. Fig. 4b shows the bottom surface of the sample A with an h2 thickness, which was obtained by sandpapering the bottom surface of the sample A. It was observed that the width of impurity regions at grain boundaries and the size of second phase particles reduced. This means that better connectivity between superconducting grains increases superconducting current [11].

Fig. 4c shows the top surface of micrograph of sample B having an h1 thickness. This sample has large Y123 grains and voids. The micrograph of the sample B with an h2 thickness (see Fig. 4d) indicates that the sizes of the voids were decreased and the sample has the non-superconducting Y211 (green phase) phases having a few μm size. These phases have spherical shapes and they are uniformly distributed. The Y211 phases were expected to work as pinning centers and hence enhance the current density [12]. In the sample A with an h3 thickness, the precipitate phases were mostly eliminated and the textured Y123 domains became larger.

Fig. 5 shows the XRD patterns of the samples A and B. The sample A-h1 presented a different XRD pattern from a typical XRD pattern of Y123. This is indeed (probably) due to the existence of preferred orientations [13] in the sample. The highest peak intensity shown in Fig. 5a was located at $2\theta \approx 46.9°$ (0 2 0) and has 14,000 (cps). The XRD pattern of the sample A-h2 exhibited the highest diffraction pattern at $2\theta \approx 40.4°$ (1 1 3) and also displayed that a peak which is not superconducting at $2\theta \approx 39.5°$ belongs to $BaCuO_2$ (see Fig. 5b).

XRD pattern from top surface of sample B-h1 states that the highest peak (Y123) about 8300 (cps) for $2\theta \approx 40.4°$ and Y211 phase peak for $2\theta \approx 29.9°$ were observed and also a preferred orientation was determined (see Fig. 5c). It can be shown from XRD pattern collected from bottom surface of sample B-h2 that the peaks belonging to superconducting phase disappeared and the non-superconducting Y211 peaks occurred as clearly seen in Fig. 5d. This result was supported by polarized light optical micrograph as shown in Fig. 4d.

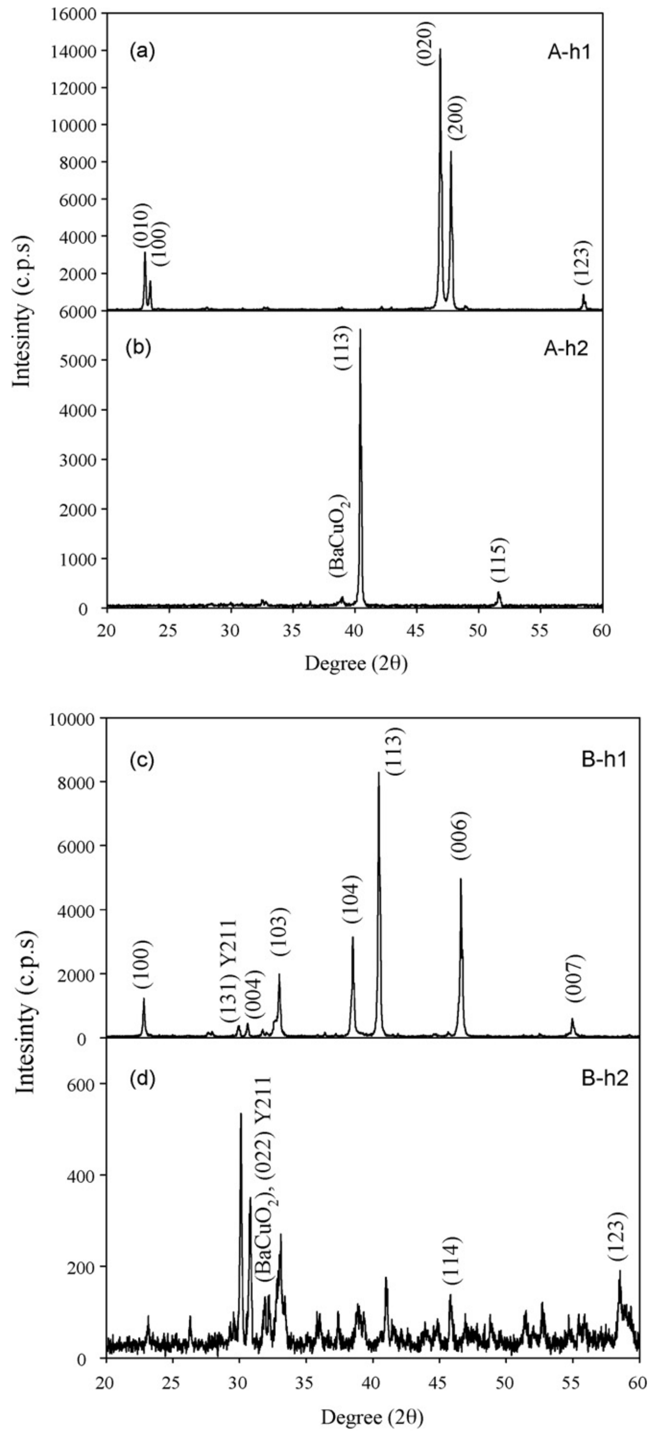

Fig. 5. XRD patterns for (a) the top surface of A-h1, (b) the bottom surface of A-h2, (c) the top surface of B-h1, and (d) the bottom surface of B-h2.

As can be clearly seen from Fig. 5, both A and B samples have impurity phases. In other words, these phases were observed to transition from h1 to h2 thickness, especially for sample B. We believe that these phases occurred during the sintering processes, i.e., a small amount of liquid leaked to the bottom of the sample and interacted with the samples.

One can expect that the sample A should have some platinum impurities, which however was not detected in the XRD measurement because the intensity of Pt peaks is very small relative to the intensity of the other peaks. On the other hand, the EDXRF measurements as shown in Fig. 6 clearly revealed the existence of Pt

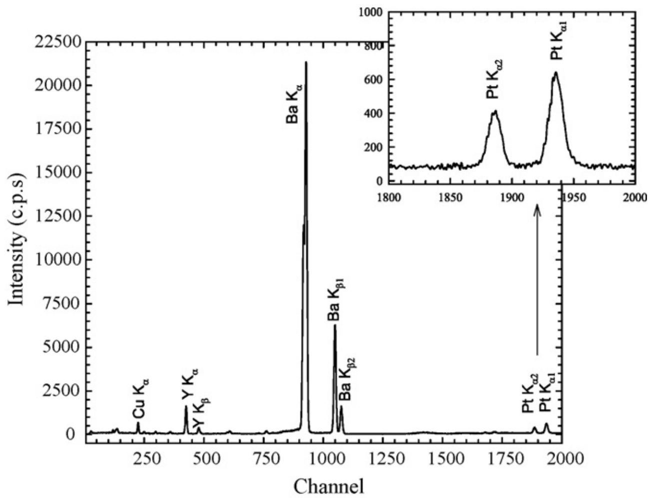

Fig. 6. EDXRF results of phases taken on after quench in MPMG.

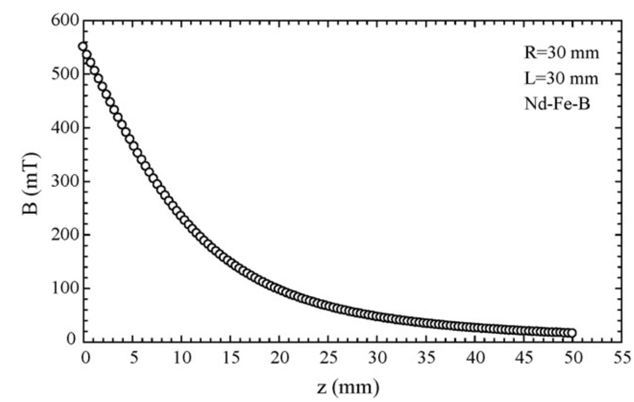

Fig. 7. Calibration curve of a standard Nd–Fe–B magnet with axially magnetic field intensity.

impurities in the sample. The rate of Pt impurities was determined to be 0.98 wt%. The influence of Pt impurities appears to be positive and they reduce to the mean size of Y211 domains in the sample. Additionally, Pt impurities produce uniform Y211 domains in the sample (see Figs. 4 and 5). It was clearly seen from the Pt-uncontaminated sample shown in Figs. 4d and 5d that the Y211 phase appeared. However, the Pt-contaminated sample shown in Fig. 5b indicates to have merged into Y211 phase in background level due to enhanced grain growth and orientation of Y123 grains. In addition, it is known that this effect increases critical current density [14,5].

Fig. 7 displays the calibration curve of a standard Nd–Fe–B magnet. The levitation force per unit volume as a function of distance was measured from the top surface of the sample A with h1, h2 and h3 thicknesses (see Fig. 8a). For the h2 thickness, only repulsive but also attractive forces noticeably increased. On the other hand, for the h3 thickness, the repulsive force decreased while the

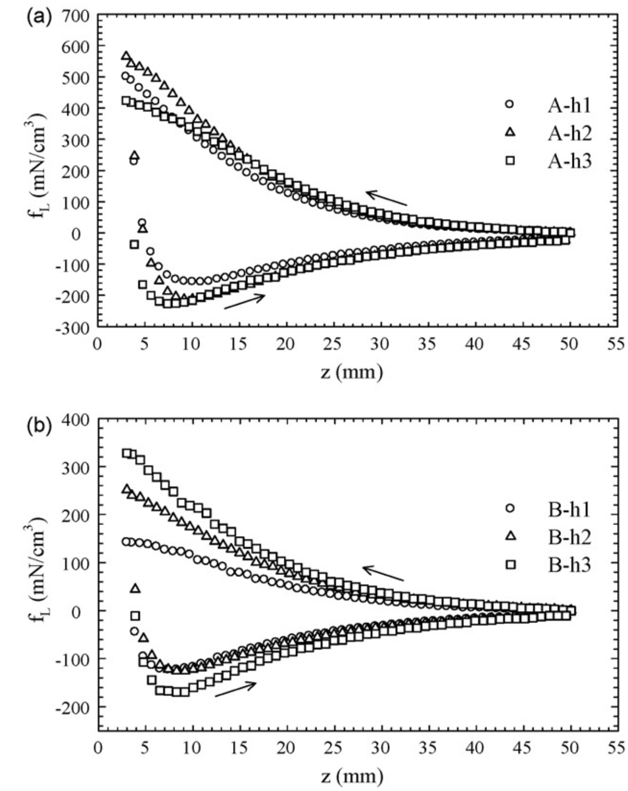

Fig. 8. Levitation force per unit superconductor volume as a function of distance *z* for different values of superconductor thickness *h* for (a) sample A and (b) sample B.

attractive force increased. The same measurement was performed for sample B and it was found that both repulsive and attractive forces increased with decreasing thickness (see Fig. 8b).

Table 1 shows the maximum values of repulsive and attractive forces for the samples A and B. Among these values, maximum repulsive force was determined to be 565 mN/cm^3 for h2 level while maximum attractive force was obtained to be 226 mN/cm^3 for h3 level for the sample A. Similarly, the maximum repulsive and attractive force values were 328 mN/cm^3 and 169 mN/cm^3 for the sample B with h3 thickness, respectively. For the comparison, when the samples A and B were compared, the levitation force for sample A was found to be higher than that of the sample B. Our finding for the sample B is in good agreement with the theoretical prediction (the previous study), which states that the levitation force per unit volume increases as thickness decreases [10]. For the sample A, however, our finding is inconsistent with Ref. [10].

During the sintering process, our superconducting sample reacted with the Al_2O_3 crucible, which resulted in significant amount of precipitate phases on the bottom part of the sample. The precipitate phases, which are not superconducting, affect negatively the levitation force. Removing precipitate phases from both samples by sandpapering (i.e., transition from h1 to h2 level), enhanced not only repulsive but also attractive forces (see Fig. 8).

Table 1
Maximum repulsive and attractive force values with relation to both melting process and thickness of superconductor.

	Samples					
	A			B		
	h1	h2	h3	h1	h2	h3
Thickness (mm)	6.2	5.5	2.5	4.1	3.8	2.3
Repulsion force (mN/cm^3)	500	565	424	142	252	328
Attractive force (mN/cm^3)	−157	−212	−226	−123	−126	−169

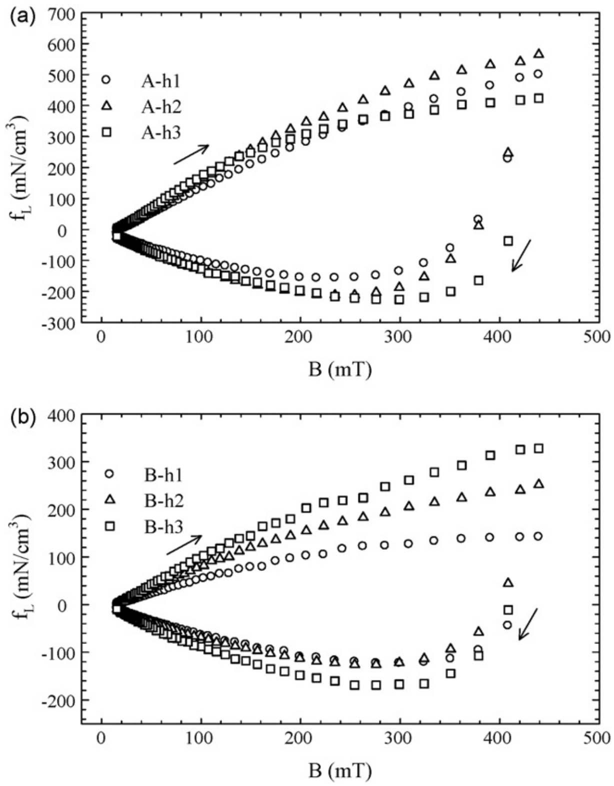

Fig. 9. Levitation force per unit superconductor volume as a function of magnetic field B for different values of superconductor thickness *h* for (a) sample A and (b) sample B.

The repulsive force beginning from h2 (i.e., transition from h2 to h3) increased from the sample B (see Fig. 8b) while it decreased for the sample A (see Fig. 8a). The change of the repulsive force in the sample B is due to the removing of the precipitate phases from the sample B, while the decrease in the levitation force in the sample A is associated with the removing of the superconducting phases from the sample A. These observations indicate that the phase of the Y123 superconductor formed predominantly on the top region of the sample B while it structured largely in the center region of the sample A.

Fig. 9 shows that levitation force per unit volume versus magnetic field for the different values of the samples' thickness. This figure was plotted by means of calibration curves since a standard magnet was used to measure the levitation force. As can be seen from the figure, the levitation force changing according to magnetic field is similar to the levitation force changing with distance. Nevertheless, the analysis in detail related to the rapid rise of the levitation force near the magnet can be done using Fig. 9. Also, levitation force values were much more discrete at regions far from magnet. Therefore, it is believed that from the plot in Fig. 9 can be enabled sensitively to analysis of levitation force. Finally, we think that this relation would help for next studies.

4. Conclusions

We fabricated YBCO samples in the stoichiometric ratio of 1:2:3 using the MPMG and FQMG processes and studied the levitation force per unit volume as a function of their thickness. It was determined from our findings that superconductivity forming ratio is sensitive to the preparation techniques and it grows (it dominates) on the surfaces of the samples prepared by FQMG method while it grows (it dominates) in the middle of the samples fabricated by MPMG method. The MPMG method produces more the superconductivity forming ratio than the FQMG method, which is due to platinum impurities. Our results were also verified by polarized optical microscope and XRD pattern.

Also, these properties should be further investigated for larger dimensional samples to enhance technological applicability. This paper related to levitation force depending on the thickness of superconducting sample and melting processes (such as MPMG, FQMG) can be very useful way for material optimization to other researchers.

Acknowledgement

This work was financially supported by the Research Fund of Karadeniz Technical University, Turkey, under grant contract no. 2005.111.001.2.

References

[1] S. Jin, T.H. Tiefel, R.C. Sherwood, R.B. van Dover, M.E. Davis, G.W. Kammlott, R.A. Fastnacht, Phys. Rev. B 37 (13) (1988) 7850.
[2] M. Murakami, M. Morita, K. Doi, K. Miyamoto, Jpn. J. Appl. Phys. 28 (1989) 1189.
[3] M. Murakami, T. Oyama, H. Fujimoto, S. Gotoh, K. Yamaguchi, Y. Shiohara, N. Koshizuaka, S. Tanaka, IEEE Trans. Magn. 27 (2) (1991) 1479.
[4] L. Zhou, P. Zhang, P. Ji, K. Wang, J. Wang, X. Wu, IEEE Trans. Magn. 27 (2) (1991) 912.
[5] M. Murakami, Supercond. Sci. Technol. 5 (1992) 185.
[6] D. Shi, S. Sengupta, J.S. Luo, C. Varanasi, P.J. McGinn, Physica C 213 (1993) 179.
[7] E. Yanmaz, I.H. Mutlu, T. Kucukomeroglu, M. Altunbas, Supercond. Sci. Technol. 7 (1994) 903.
[8] S. Sagar, K. Lahiri, D. Shi, IEEE Trans. Appl. Supercond. 7 (2) (1997) 1929.
[9] C. Leblond, I. Monot, D. Bourgault, G. Desgardin, Supercond. Sci. Technol. 12 (1999) 405.
[10] M.K. Alqadi, H.M. Al-khateeb, F.Y. Alzoubi, N.Y. Ayoub, Chin. Phys. Lett. 24 (9) (2007) 2664.
[11] K. Salama, D.F. Lee, Supercond. Sci. Technol. 7 (1994) 177.
[12] A. Gencer, A. Ateş, E. Aksu, S. Nezir, S. Celebi, E. Yanmaz, Physica C 279 (1997) 165.
[13] E. Yanmaz, S. Balci, T. Küçükömeroğlu, Mater. Lett. 54 (2002) 191.
[14] N. Ogawa, I. Hirabayashi, S. Tanaka, Physica C 177 (1991) 101.